Materials Chemistry and Physics 115 (2009) 313–321

Contents lists available at ScienceDirect

Materials Chemistry and Physics

journal homepage: www.elsevier.com/locate/matchemphys

Carbon steel passivity examined in solutions with a low degree of carbonation: The effect of chloride and nitrite ions

M.B. Valcarce, M. Vázquez*

División Corrosión, INTEMA, Facultad de Ingeniería, UNMdP, Juan B. Justo 4302 - B7608FDQ Mar del Plata, Argentina

ARTICLE INFO

Article history:
Received 2 June 2008
Received in revised form 4 November 2008
Accepted 8 December 2008

Keywords:
Surfaces
Oxides
Electrochemical techniques
Corrosion

ABSTRACT

The effect of nitrite ions as inhibitors against steel corrosion in carbonated and chloride-contaminated concrete pore simulating solutions (pH 9) is investigated. Various inhibitor dosages and two chloride contents are tested. The inhibition efficiency is evaluated measuring the corrosion potential, cyclic voltammograms, anodic polarization curves, pitting and repassivation potentials, polarization resistance and performing electrochemical impedance spectra, together with weight-loss measurements. Independently of the chloride content, when $[NO_2^-] = 0.2\ mol\ l^{-1}$, the inhibition efficiency reaches 99% and if pitting occurs, surface repassivation is possible. At high chloride contents, if inadequate dosages of inhibitor are used, the risk of pitting attack is high because E_{pit} is close to the OCP. The $[NO_2^-]/[Cl^-]$ ratio is not an appropriated parameter to evaluate the inhibitor efficiency for varying chloride concentrations in a carbonated concrete. An optimal nitrite ions concentration ($[NO_2^-] = 0.2\ mol\ l^{-1}$) can be established as the most suitable parameter to guarantee the inhibitor efficiency in the different electrolytes studied.

1. Introduction

Reinforced concrete is one of the most important structural materials used in the construction industry worldwide, due mainly to low cost, availability and formability, coupled to excellent structural and durability properties. However, aggressive service environments and contaminated aggregates can contribute to its early deterioration and failure. One of the main factors that negatively influences the performance of reinforced concrete is the corrosion of the steel bars.

In the case of good quality concrete, the high alkalinity in the pore solution determines the development of an oxide layer that protects the steel against active corrosion: the metal remains passive with a very low corrosion rate. Unfortunately, in the presence of aggressive agents, the passive layer on steel is damaged and the rebar corrosion rate can become significant. Rebar corrosion may occur as a result of concrete alkalinity loss due to CO_2 diffusion, of the presence of aggressive ions (mainly chlorides), or due to a combination of these factors [1,2].

To minimize the effect of rebar corrosion, various techniques are frequently employed, such as cathodic protection, inhibitors, and the application of coatings to the external concrete surface or to the reinforcing steel bars.

Nitrite ions are well-known corrosion inhibitors of steel corrosion in concrete [2,3]. However, in marine environments or when concrete is prepared with contaminated aggregates, the presence of chloride ions can decrease the inhibitor efficiency. Chloride ions can penetrate the porous structure of concrete from marine environments. On top of this, in many coastal cities in Argentina, the use of seasand and chloride-contaminated coarse aggregates and water constitutes a recurrent malpractice.

The corrosion risk associated to a certain chloride content is usually evaluated in terms of the chloride/hydroxyl ratio [4]. Alternatively, nitrite ions as inhibiting agents in the presence of chloride are evaluated as a function of the nitrite/chloride ratio. There is no clear agreement on the threshold value of this ratio. Values ranging from 0.34 to more than 1 have been given by different authors [1,5–7] as those necessary to prevent corrosion in concrete.

In good quality, non-contaminated concrete, the high alkalinity of the electrolyte guarantees steel passivation even in the presence of chlorides. It has been shown before [8] that even if the passive layer is damaged and pitting is initiated, nitrite ions are effective in inhibiting pit propagation. A nitrite/chloride ratio of 0.25 induces complete surface repassivation.

The investigation of the corrosion of steel in concrete has special challenges because one has to deal with highly resistive and porous materials. On the other hand, appropriated solutions can simulate the chemical environment present in the concrete pores. Many authors have employed highly carbonated solutions to reproduce the pore solutions in carbonated concrete when carrying out corrosion studies [9–11]. However, the real pore solution presents a

* Corresponding author. Tel.: +54 223 481 6600; fax: +54 223 481 0046.
E-mail address: mvazquez@fi.mdp.edu.ar (M. Vázquez).

0254-0584/$ – see front matter © 2008 Elsevier B.V. All rights reserved.
doi:10.1016/j.matchemphys.2008.12.007

low concentration of soluble carbonate and bicarbonate ions when carbonated concrete specimens were analyzed using the pore solution expression test [12,13]. Also, it has been suggested that the $CO_3^{=}$ and HCO_3^{-} contents could influence the properties of the surface layer [14,15].

The results to be presented below address the effect of nitrite ions on the breakdown of passive films formed on steel reinforcements in an electrolyte that simulates the solution present in chloride-contaminated and carbonated concrete pore solutions. In this case, pH is reduced to 9 due to the penetration of carbon dioxide through the pores in concrete. This condition will be used as reference for a work in progress where we are evaluating the effect of high carbonate and bicarbonate concentrations on the inhibitor efficiency.

2. Experimental

2.1. Electrolyte composition

The present investigation was carried out in solutions with a low degree of carbonation (CS), to simulate the composition of the solution contained in the pores of carbonated concrete. The electrolyte contains Na_2CO_3 0.0015 mol l^{-1} and $NaHCO_3$ 0.03 mol l^{-1} with a resulting pH value of 9 [15,16].

The nitrite ions content was chosen as 0.2 mol l^{-1} from the work of Li et al. [17] and Berke and Hicks [7], as explained in detail before [8]. Taking this as a reference value various concentrations of $NaNO_2$ were added to the CS solution in order to evaluate the inhibitor effect, as conveniently indicated.

To simulate a concrete which further than being carbonated is also contaminated with chloride ions, CS solutions incorporate two different amounts of NaCl: CS + 1 × 10^{-3} mol l^{-1} NaCl resulting in $[Cl^-]/[OH^-] = 100$) or CS + 0.1 mol l^{-1} NaCl (so that $[Cl^-]/[OH^-] = 1 \times 10^4$).

2.2. Electrodes preparation

Samples were prepared from steel reinforcement bars (Mn 0.635%, C 0.299%, Si 0.258%, Cu 0.227% and others impurities 0.245%). Disks with a geometrical area of 0.503 cm^2 were prepared mounting a back electrical contact, included in fast curing acrylic resin on appropriated PVC holders and polished down to grade 1000 with emery paper.

2.3. Electrochemical techniques

A conventional electrochemical set-up was used, as described elsewhere [8]. All the potentials are indicated against a Hg/HgO/KOH (1 mol l^{-1}) reference, labelled as MOE, $E = 0.123$ V vs. NHE.

All the experiments were carried out with a Voltalab PGP 201 potentiostat.

Cyclic voltammograms were recorded after deaerating the electrolyte by bubbling N_2 during 15 min prior to each measurement. The electrodes were pre-reduced at −1.1 V for 5 min. Finally, the scan was started at −1.1 V and reversed at 0.50 V or at convenient potential values, as indicated. The sweep rate used was 0.01 V s^{-1}.

Polarization resistance (R_p) was evaluated as $\Delta V/\Delta j$, from potential sweeps scanning ±0.01 V from the OCP at a scan rate of 1 × 10^{-4} V s^{-1}. Average values of over five individual experiments were obtained in the case of samples aged for 1 day. The corrosion rate was evaluated from Stern–Geary relationship as indicated previously [8,18].

Anodic polarization curves were recorded on electrodes with 24 h of ageing at the OCP. The curves started at OCP and were recorded at 1 × 10^{-4} V s^{-1}. Then, the scan direction was reversed at 4 × 10^{-5} A cm^{-2}. This value was chosen to induce a convenient degree of attack. The overall procedure follows the recommendations of ASTM [19].

2.4. Electrochemical impedance spectroscopy

Electrochemical impedance spectroscopy (EIS) tests were performed at open circuit potential (OCP) after 1 day of ageing. The amplitude of the AC voltage signal was ±0.01 V while the frequency varied between 20 kHz and 1 mHz. The results were analyzed using two different equivalent circuits: a Randles circuit, in the case of active dissolution, as well as the circuit presented in Fig. 1. This circuit is typical of oxide-coated metals and has been used before by other authors [8,20,21]. The experimental data were fitted to the proposed equivalent circuit using ZView™ [22]. Corroding electrodes can show various types of inhomogeneities, which can be represented by the inclusion of constant phase elements (CPE) replacing the capacitors in the equivalent circuit. Surface roughness, insufficient polishing, grain boundaries and surface impurities had been mentioned before among the main reasons allowing the use of CPEs in equivalent circuits of corroding electrodes [23]. The impedance of this element is frequency-dependent, and can be mathematically expressed using

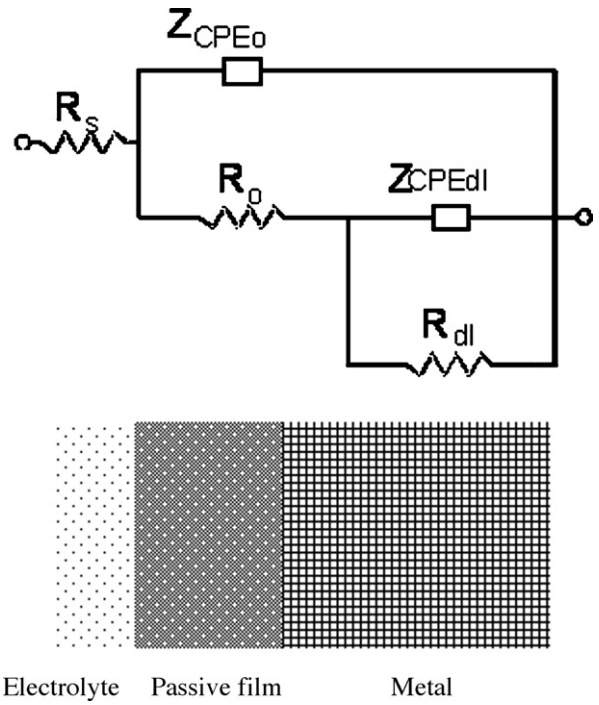

Fig. 1. Equivalent circuit proposed to fit the experimental data when two time constants are present.

two parameters, Q and n as:

$$Z_{CPE} = [Q(j\omega)^n]^{-1} \quad (1)$$

where Q is a constant with dimensions of Ω cm^2 $s^{-(1-n)}$ and n a constant power, with $-1 < n < 1$. According to the value of n, Eq. (1) accounts for an inductance ($n = -1$), a resistance ($n = 0$), a Warburg impedance ($n = 0.5$) or a capacitance ($n = 1$). A rough or porous surface can cause a double layer capacitance to appear as a constant phase element with n varying between 0.5 and 1.

2.5. Surface analysis

Coupons polished down to grade 1000 with emery paper were immersed in the test solutions for 7 days at OCP. The containers were kept at room temperature, with gentle agitation to avoid differential deaeration. Then, coupons were withdrawn, rinsed with distilled water and dried with ethanol, under N_2 atmosphere.

The morphology of the passive layer was examined by scanning electron microscopy (SEM), using a JEOL JSM-6460LV microscope.

The composition of the passive layer was analyzed by energy dispersive X-ray spectroscopy (EDX) investigations. The system used was an EDAX Genesis XM4—Sys 60, equipped with Sapphire Si(Li) detector and Super Ultra Thin Window of Be.

2.6. Weight-loss determinations

The Weight Loss Method was applied following the guidelines in ASTM D 2688 Standard Test Methods for Corrosivity of Water in the Absence of Heat Transfer. Coupons in the shape of disks with a geometrical area of 7.22 cm^2 were cut and polished down to grade 120 with emery paper.

After weighting them, the coupons were suspended and immersed in the different test solution as is indicated in Table 4, placing five coupons in each of ten containers. The containers were kept at room temperature, with gentle agitation to avoid differential deaeration. The coupons were withdrawn from each container after 30 days. The corrosion products were dissolved with HCl 10%. Then the samples were neutralized with saturated Na_2CO_3 solution, and rinsed with distilled water, to be finally dried, weighted and examined with a metallographic microscope.

3. Results and discussion

The cyclic voltammogram of steel in contact with deaerated carbonated solutions (CS, pH 9) is shown in Fig. 2. The results are compared with the voltammogram obtained in highly alkaline solution (AS) with pH 13.9 without carbonate or bicarbonate ions [8].

Oxide growth starts at −1.10 V in AS. A sharp anodic peak is evident at −0.72 V (Ia), together with a shoulder at −0.36 V (IIa).

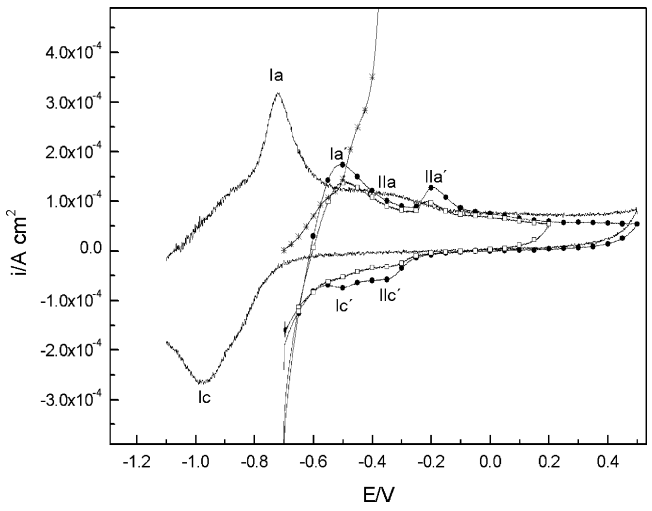

Fig. 2. Cyclic voltammogram of carbon steel in deaerated AS (—), CS (×), CS + 0.2 mol l^{-1} $NaNO_2$ (●) and CS + 0.2 mol l^{-1} $NaNO_2$ + 0.1 mol l^{-1} NaCl (□). Scan rate: 1×10^{-2} V s^{-1}.

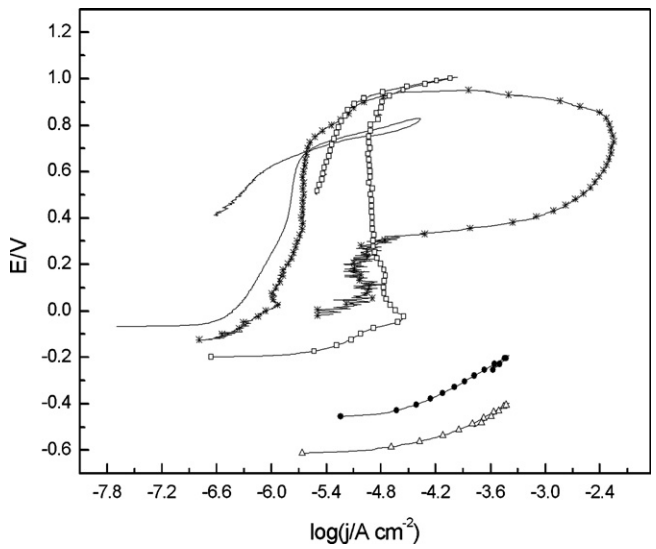

Fig. 3. Anodic polarization curves for carbon steel in CS + 1×10^{-3} mol l^{-1} NaCl ([Cl$^-$]/[OH$^-$] = 100). With [NO_2^-] = 0.2 mol l^{-1} or [NO_2^-]/[Cl$^-$] = 200 (—), [NO_2^-] = 0.025 mol l^{-1} or [NO_2^-]/[Cl$^-$] = 25 (×), [NO_2^-] = 0.0025 mol l^{-1} or [NO_2^-]/[Cl$^-$] = 2.5 (□), [NO_2^-] = 2.5×10^{-4} mol l^{-1} or [NO_2^-]/[Cl$^-$] = 0.25 (●) and [NO_2^-]/[Cl$^-$] = 0 (△). The curves were recorded after holding the electrodes 24 h at OCP and each started at OCP. Scan rate: 1×10^{-4} V s^{-1}.

The processes associated to the anodic peaks can be attributed to Fe(III)-containing compounds such as Fe_3O_4 and δ-FeOOH, as reported before [24,25]. Changing the limits of the potential window, it can be seen that both anodic processes are associated to a single cathodic peak at −0.98 V (Ic).

In CS the current density increases continuously with potential and no passivation plateau can be observed. An increment in CO_3^{2-} ions could favor the development of a passive film on the metal surface [15,16,26] and hinder pitting because of their buffering capacity, thus preventing local acidification [16,27].

As can be seen in Fig. 2, in CS + [NO_2^-] = 0.2 mol l^{-1} a steady-state current typical of passivity is reached. In this condition, the anodic current starts to grow at potentials higher than −0.6 V. Two oxidation peaks appear at −0.51 V (Ia′) and −0.19 V (IIa′). Changing the potential limits, it can be seen that the anodic peak Ia′ is associated to the cathodic peak Ic′ at −0.50 V and the anodic peak IIa′ is related to the cathodic peak IIc′ at −0.35 V. These potentials could be attributed to compounds containing Fe(III) (as in AS), in agreement with the Pourbaix diagram for iron (Fe/H_2O), because the position of the peaks depends on the pH value [26,28]. There is no evidence of localized corrosion.

The negative effect of chloride ions on the passive layer naturally formed on iron exposed to alkaline environments has been extensively reported in the literature. The chloride threshold values for the corrosion of steel in concrete, mortars and highly alkaline solutions have been investigated by many authors [4,24,29–31]. In highly alkaline solutions the threshold value relative to the OH$^-$ content, given as [Cl$^-$]/[OH$^-$] ratio presents a mean value around 0.6 [32,33].

Thus, a sequence of polarization curves with [NO_2^-] = 0.2 mol l^{-1} was carried out in a solution contaminated with varying amounts of chloride ions and after keeping the electrodes at OCP for 24 h. Low chloride concentrations such as 1×10^{-5} mol l^{-1} ([Cl$^-$]/[OH$^-$] = 1) produced no significant differences in the polarization curves when they were compared with those in CS + [NO_2^-] = 0.2 mol l^{-1} free of chloride ions. So, conditions where [Cl$^-$]/[OH$^-$] = 100 ([NaCl] = 1×10^{-3} mol l^{-1}) and [Cl$^-$]/[OH$^-$] = 1×10^4 ([NaCl] = 0.1 mol l^{-1}) were also tested.

When both nitrite ([NO_2^-] = 0.2 mol l^{-1}) and chloride ions are present in solution, no significant differences were observed in the position and intensity of the anodic peaks in the cyclic voltammogram (Fig. 2) which could be attributed to the presence of chlorides. However, the potential scan has to be reversed at 0.2 V to avoid pitting when [NaCl] = 0.1 mol l^{-1}.

The effect of varying the nitrite dosage was evaluated comparing the anodic polarization curves performed on samples aged during 24 h at OCP. The curves were recorded in carbonated solutions with a chloride concentration of 1×10^{-3} mol l^{-1} and nitrite/chloride ratios ranging between 0.25 and 200, as presented in Fig. 3. Some relevant electrochemical parameters such as passivity currents (j_{pas}), corrosion potential (E_{corr}), pitting potentials (E_{pit}) and repassivation potentials (E_{rp}) were calculated from the anodic polarization curves. These results are presented in Table 1. In the case of the uninhibited solution and when the nitrite/chloride ratio equals 0.25, steel undergoes general corrosion. Even though the current decreases about one order of magnitude in the presence of nitrites, a continuously increasing current is registered, which is typical of active dissolution processes. When more nitrite is incorporated, so that [NO_2^-]/[Cl$^-$] = 2.5, a limiting current close to 5×10^{-6} A cm^{-2} is attained, that could be associated to a diffusion

Table 1
Relevant electrochemical parameters, characteristic of the anodic polarization curves in carbon steel after 24 h of immersion in CS + 1×10^{-3} mol l^{-1} NaCl ([Cl$^-$]/[OH$^-$] = 100).

[NO_2^-] (mol l^{-1}), in CS [Cl$^-$]/[OH$^-$] = 100	0.2	0.025	2.5 × 10−3	2.5 × 10−4	0
[NO_2^-]/[Cl$^-$]	200	25	2.5	0.25	0
E_{corr} (mV)	−85	−99	−212	−401	−513
E_{pit} (mV)	716	768	–	–	–
E_{rp} (mV)	665	–	–	–	–
j_{pas} (A cm^{-2})	1.7×10^{-6}	2.3×10^{-6}	–	–	–
$E_{pit} - E_{corr}$ (mV)	801	867	–	–	–
R_p (kΩ cm^2)	331	233	17.2	1.74	1.64
Inhibition%	99.6	99.4	91.8	18.9	–

process through a non-protective thick film of corrosion products [16]. No evidence of a defined pitting potential was found. Only in the case of higher nitrite concentrations, as when $[NO_2^-]/[Cl^-] = 25$, the limiting current approaches 1×10^{-6} A cm^{-2}, which is a value typical of a passive surface [8,30]. In this case pitting occurs but after pitting, there is no sign of repassivation in the reverse potential scan. Surface repassivation seems to be possible only when $[NO_2^-] = 0.2$ mol l^{-1} ($[NO_2^-]/[Cl^-] = 200$).

At OCP the reversible formation of Fe(OH) adsorbed on the bare metal is the first stage of the passivation process followed by the oxidation of this layer to produce a passivating oxide film [34,35]. The presence of nitrite ions could favor the oxidation process [10] following a processes that can be summarized as [8]:

$$4Fe(OH)_{2\,s} + 2NO_2^- \rightarrow N_2O + 4FeOOH_s + 2HO^- + H_2O \quad (2)$$

At highly positive potentials, the presence of chloride ions induces pitting attack. Passivity breakdown of carbon steel is influenced by the balance between two processes competing on the metal surface: stabilization of the passive film by OH^- adsorption and disruption of the film by Cl^- ions adsorption. Pitting starts when the effect of chlorides overcomes that of hydroxyls [4,24]. Due to the presence of adequate dosages of nitrite ions in the electrolyte, repassivation starts as soon as the potential sweep is reverted. The hard and soft acids and bases principle (HSAB) can be used to explain the inhibition of pit growth [36]. In this context, NO_2^- is acting as a soft base by chemisorpting on the bare iron substrate, displacing chloride ions inside of the pit.

Also, R_p values measured at OCP prior to recording each curve are indicated in Table 1. As expected, an increment in the nitrite content is related to an increment in the OCP and higher R_p values. It can be seen that the percentage of inhibition, measured as

$$\text{Inhibitor\%} = \left[1 - \left(\frac{R_p \text{ without inhibitor}}{R_p \text{ with inhibitor}}\right)\right] \times 100 \quad (3)$$

exceeds 99% for the two higher nitrite contents. However, high inhibitor efficiencies do not necessarily guarantee surface repassivation if the passive layer is damaged. In the case of rebars in service conditions, this is an unlikely event since the difference between the pitting and the open circuit potential is very big.

The influence of the nitrite content on the inhibition process has also been investigated in heavily chloride-contaminated solutions. The anodic polarization curves performed on samples aged during 24 h at open circuit potential in carbonated solutions with a chloride concentration of 0.1 mol l^{-1} and nitrite/chloride ratios ranging between 0.25 and 2 are presented in Fig. 4. Table 2 shows some relevant electrochemical parameters calculated from the anodic polarization curves in Fig. 4. In this case, even the smallest addition of nitrite ions (namely 0.025 mol l^{-1}) prevents the electrode from being in active dissolution, with a percentage inhibition as high as 91.4%. Then, as the nitrite increases, the passivity current decreases and the pitting potential moves slowly to more positive values [9–11,37] together with an increment in the OCP. Again, surface repassivation does only seem to be possible in the highest nitrite concentration evaluated (0.2 mol l^{-1}). In the case of a higher chloride content, the risk of pitting cannot be disregarded, because the difference between the pitting and the open circuit potential is small.

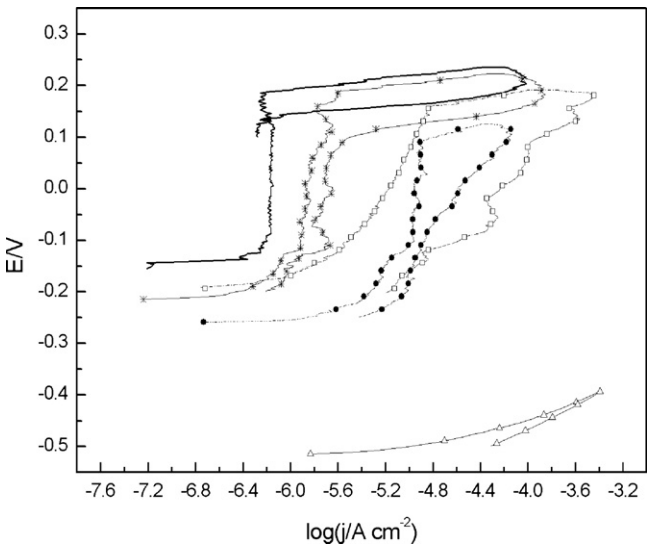

Fig. 4. Anodic polarization curves for carbon steel in CS + 0.1 mol l^{-1} NaCl ($[Cl^-]/[OH^-] = 1 \times 10^4$). With $[NO_2^-] = 0.2$ mol l^{-1} or $[NO_2^-]/[Cl^-] = 2$ (—), $[NO_2^-] = 0.1$ mol l^{-1} or $[NO_2^-]/[Cl^-] = 1$ (×), $[NO_2^-] = 0.05$ mol l^{-1} or $[NO_2^-]/[Cl^-] = 0.5$ (□), $[NO_2^-] = 0.025$ mol l^{-1} or $[NO_2^-]/[Cl^-] = 0.25$ (●) and $[NO_2^-]/[Cl^-] = 0$ (△). The curves were recorded after holding the electrodes 24 h at OCP and each started at OCP. Scan rate: 1×10^4 V s^{-1}.

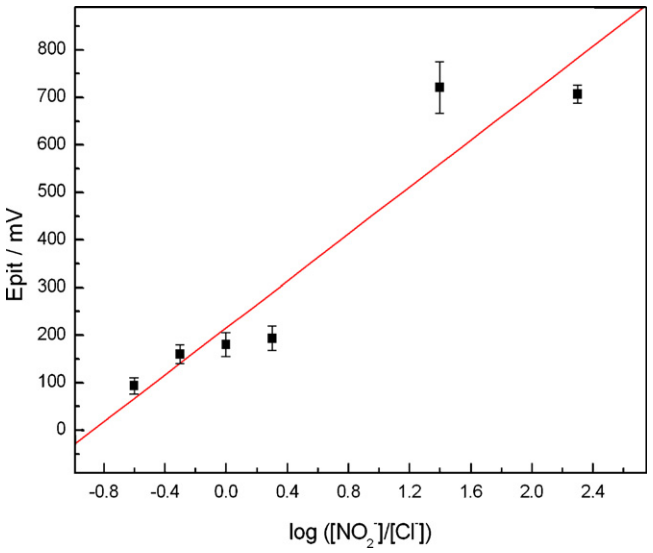

Fig. 5. Logarithmic relationship between the pitting potential (E_{pit}) and the $[NO_2^-]/[Cl^-]$ ratio.

Table 2
Relevant electrochemical parameters, characteristic of the anodic polarization curves in carbon steel after 24 h of immersion in CS + 0.1 mol l^{-1} NaCl ($[Cl^-]/[OH^-] = 1 \times 10^4$).

$[NO_2^-]$ (mol l^{-1}), in CS $[Cl^-]/[OH^-] = 1 \times 10^4$	0.2	0.1	0.05	0.025	0
$[NO_2^-]/[Cl^-]$	2	1	0.5	0.25	0
E_{corr} (mV)	−131	−206	−193	−228	−533
E_{pit} (mV)	193	180	161	95	–
E_{rp} (mV)	145	–	–	–	–
j_{pas} (A cm^{-2})	7.2×10^{-7}	1.4×10^{-6}	4.9×10^{-6}	1.2×10^{-5}	–
$E_{pit} - E_{corr}$ (mV)	324	340	354	323	–
R_p (kΩ cm^2)	216	186	53	18	1.49
Inhibition%	99.3	99.2	97.1	91.4	–

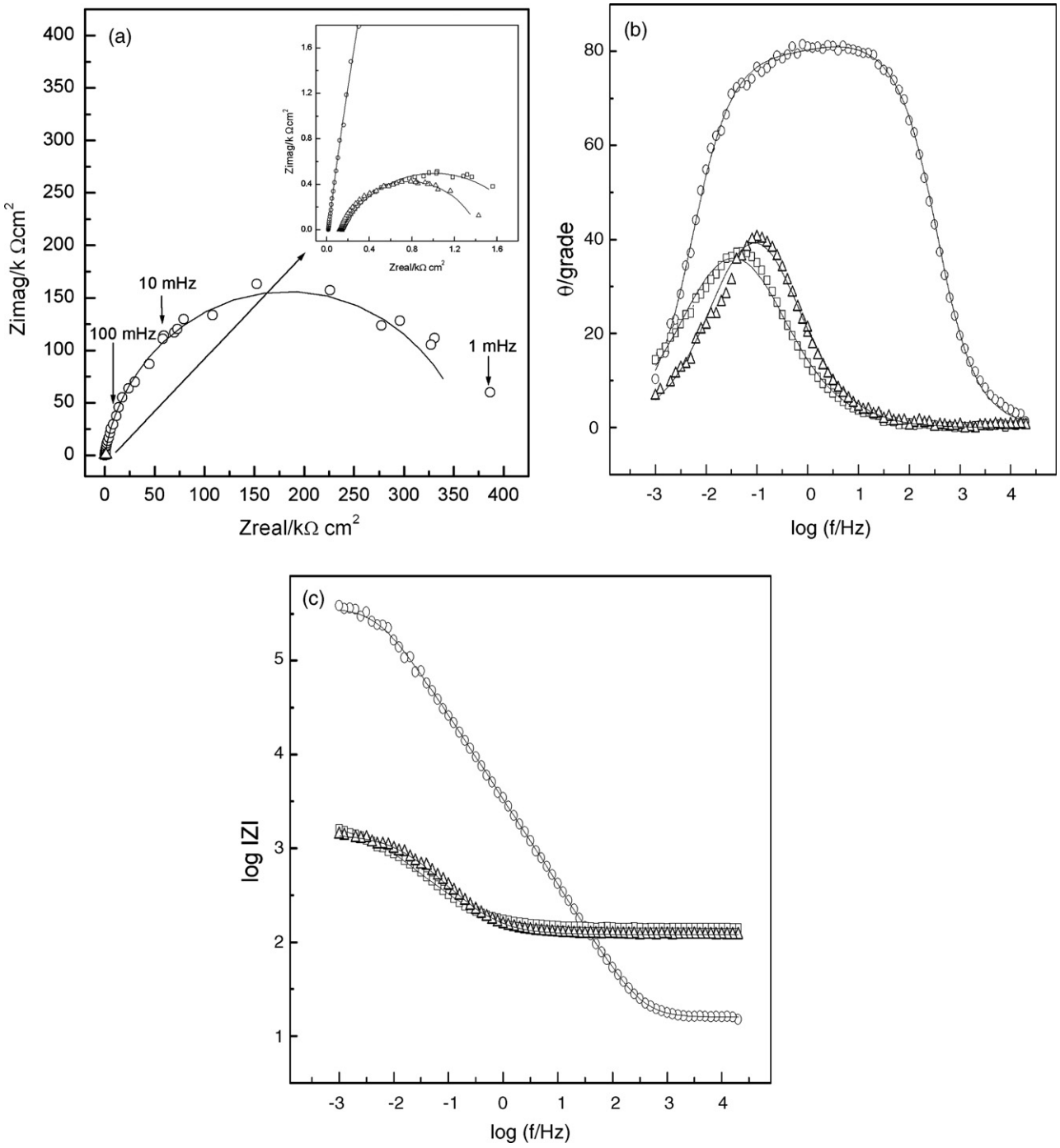

Fig. 6. Impedance spectra recorded on carbon steel electrodes held for 24 h at OCP in CS + 1×10^{-3} mol l^{-1} NaCl ($[Cl^-]/[OH^-] = 100$). With $[NO_2^-] = 0.2$ mol l^{-1} or $[NO_2^-]/[Cl^-] = 200$ (○), $[NO_2^-] = 2.5 \times 10^{-4}$ mol l^{-1} or $[NO_2^-]/[Cl^-] = 0.25$ (□) and $[NO_2^-]/[Cl^-] = 0$ (△). The symbols represent the data and the lines the fitting results. (a) Nyquist representation; (b) and (c) Bode representation.

The relationship between the pitting potential (E_{pit}) and the inhibitor concentration (C_{inh}) depends on the following equation in the presence of an aggressive anion (C_a) [38]:

$$E_{pit} = a + b \log\left(\frac{C_{inh}}{C_a}\right) \quad (4)$$

Fig. 5 shows the linearity between E_{pit} and $\log([NO_2^-]/[Cl^-])$. The values of a and b can be obtained from this plot, resulting in $a = 215$ mV and $b = 247$ mV per decade. This relationship enables the estimation of E_{pit} for a given $[NO_2^-]/[Cl^-]$ ratio.

The impedance spectra recorded using electrodes aged during 24 h with $[Cl^-] = 1 \times 10^{-3}$ mol l^{-1} or $[Cl^-]/[OH^-] = 100$ and two different concentration of nitrite ions are shown in Fig. 6 in the form of Nyquist and Bode plots. The impedance spectra were fitted with a classical Randles circuit when $[NO_2^-]/[Cl^-]$ equals 0 and 0.25, where the metal surface undergoes general corrosion. When $[NO_2^-]/[Cl^-] = 200$ a second time constant at higher frequencies appears in the Bode plot (Fig. 6b), indicating the development of a passive layer and then the spectra can be fitted using the equivalent circuit in Fig. 1. The values for the relevant parameters are presented in Table 3. In the equivalent circuit proposed R_s is the electrolyte resistance, the term R_o represents the ohmic resistance of the electrolyte through the film and the term Z_{CPE0} represents the film capacitance. R_o is in series with a parallel arrangement of the

Table 3
Optimized parameters fitting data in Figs. 6 and 7 to the classical Randles circuit (one time constant) or to the equivalent circuit proposed in Fig. 1 (two time constants).

$[NO_2^-]$ (mol l^{-1}), in CS	$[Cl^-]/[OH^-] = 100$			$[Cl^-]/[OH^-] = 1 \times 10^4$		
	0	2.5×10^{-4}	0.2	0	0.025	0.2
$[NO_2^-]/[Cl^-]$	0	0.25	200	0	0.25	2
R_s (Ω cm^2)	120	141	16	32	19	13
Q_0 (Ω^{-1} cm^{-2} S^N)	–	–	5.3×10^{-5}	–	1.9×10^{-4}	5.7×10^{-5}
n_o	–	–	0.92	–	0.82	0.91
R_o (Ω cm^2)	–	–	45,861	–	3,338	55,552
Q_{dl} (Ω^{-1} cm^{-2} S^N)	4×10^{-3}	5.7×10^{-3}	6.92×10^{-6}	5.2×10^{-3}	2.4×10^{-4}	3.5×10^{-5}
n_{dl}	0.73	0.66	0.75	0.72	0.58	0.56
R_{dl} (Ω cm^2)	1307	1737	323,260	1511	17,605	353,530

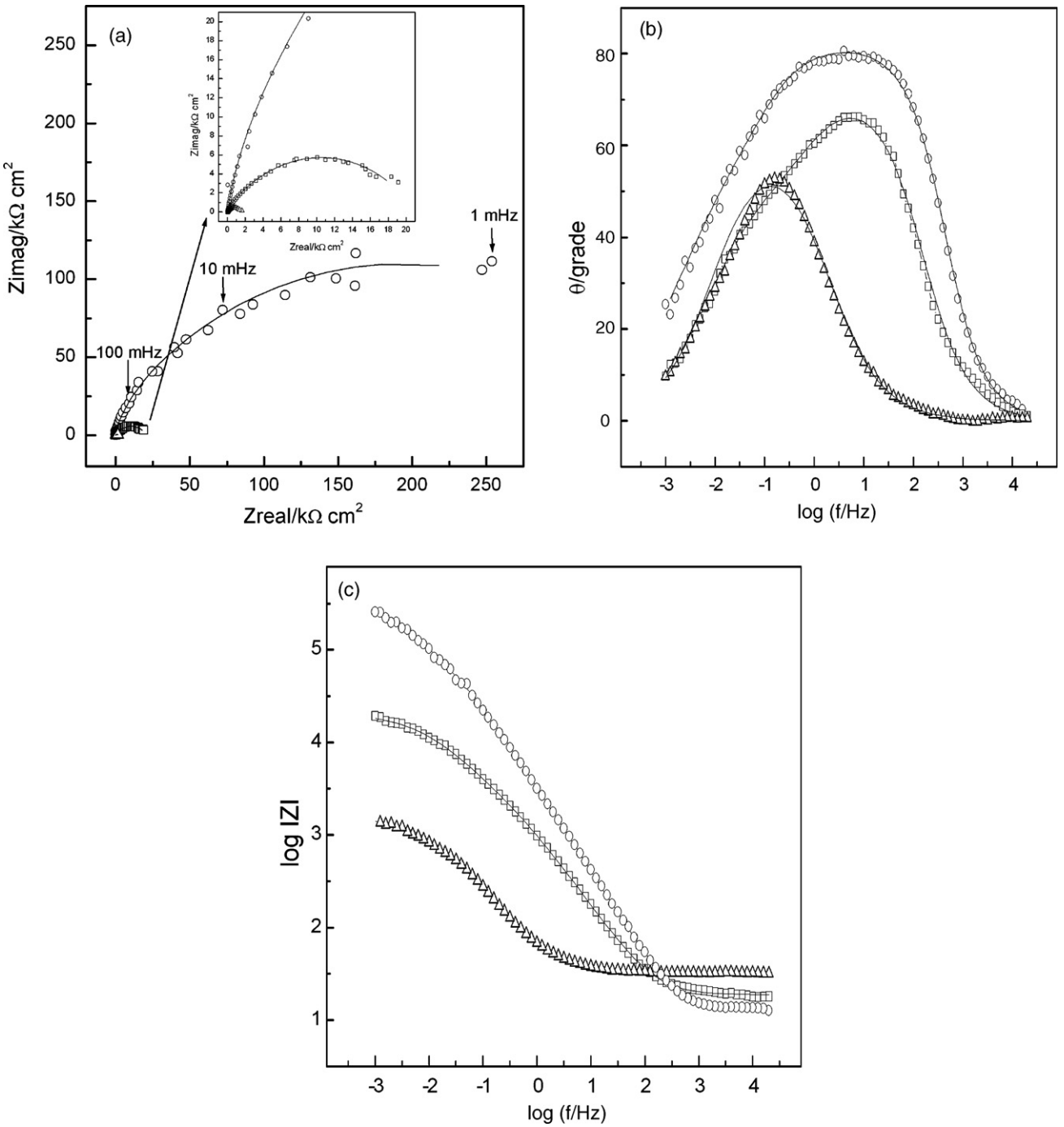

Fig. 7. Impedance spectra recorded on carbon steel electrodes held for 24 h at OCP in CS + 0.1 mol l^{-1} NaCl ($[Cl^-]/[OH^-] = 1 \times 10^4$). With $[NO_2^-] = 0.2$ mol l^{-1} or $[NO_2^-]/[Cl^-] = 2$ (○), $[NO_2^-] = 0.025$ mol l^{-1} or $[NO_2^-]/[Cl^-] = 0.25$ (□) and $[NO_2^-]/[Cl^-] = 0$ (△). The symbols represent the data and the lines the fitting results. (a) Nyquist representation; (b and c) Bode representation.

double layer capacitance Z_{CPEdl} and the Faradaic branch consisting of a charge transfer resistance R_{dl}.

The R_{dl} values are in agreement with the R_p values presented in Table 1, while C_{dl} is within the range of values commonly accepted for double layers on bare metals [26,39]. If Q_0 (Eq. (1)) is taken as the pseudo-capacitance associated with the oxide layer and approximated by the following expression for a flat plate condenser:

$$Q_0 = \frac{\varepsilon\varepsilon_o}{\delta} \quad (5)$$

where ε is the dielectric constant of the material and ε_o the permittivity of vacuum (8.8542×10^{-14} F cm^{-1}), the film thickness (δ) could be calculated. However, taking ε as 30 [40], the film thickness results lower than 1 nm. Even accepting that the film cannot be represented by an ideal capacitor and that the active area is surely different from the geometrical area, this is a somewhat surprising result as the thickness value is lower than the 1–5 nm range reported by other authors in similar conditions [26,41,42].

The impedance spectra recorded using electrodes aged during 24 h with [NaCl] = 0.1 mol l^{-1} or [Cl$^-$]/[OH$^-$] = 1×10^4 and two different concentration of nitrite ions are shown in Fig. 7. The impedance spectra were fitted with a classical Randles circuit when [NO_2^-]/[Cl$^-$] = 0 and the metal surface undergoes in general corrosion. When the [NO_2^-]/[Cl$^-$] ratios are 0.25 and 2, the spectra were fitted again using the equivalent circuit in Fig. 1. The optimized values for the various parameters are presented in Table 3. An increment of R_o together with a lower Q_0 could be associated to the development of a thicker and more compact passive layer on the electrode surface when the inhibitor content increases [20]. Again, R_{dl} values are in agreement with the R_p values presented in Table 2.

As can be seen, when [NO_2^-] = 0.2 mol l^{-1}, Q_0, Q_{dl} and R_o did not show significant differences when the chloride ions content increases in the test solution, suggesting that no changes occur in the density or thickness of the passive layer. Also, the limitations mentioned above as regards the calculation of the thickness still apply in this condition.

It is interesting to observe that the circuit proposed in Fig. 1 has also been used by other authors to discuss passive layers formation on iron in contact with mortars or alkaline solutions [43,44]. In those cases, the low-frequency time constant has been attributed to the occurrence of oxidation–reduction process on the electrode. However, the capacitances reported by these authors are much higher than those in this system (roughly 1–100 mF cm^{-2}) and the impedance spectra are registered under polarization, where different redox reactions occur, depending on the applied potential.

Figs. 8 and 9 show the EDX spectra (with an intensity of 3 and 15 kV) together with the scanning electron microscopy examination, after keeping the carbon steel surface in CS with [NO_2^-] = 0.2 mol l^{-1} for 7 days at OCP. In highly carbonated solutions, the presence of a high intensity single peak of oxygen three

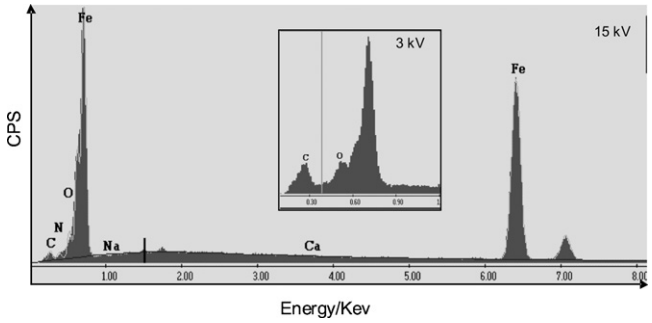

Fig. 8. Energy dispersive X-ray (EDX) spectra (3 and 15 kV), after 7 days in CS + [NO_2^-] = 0.2 mol l^{-1} at open circuit potential.

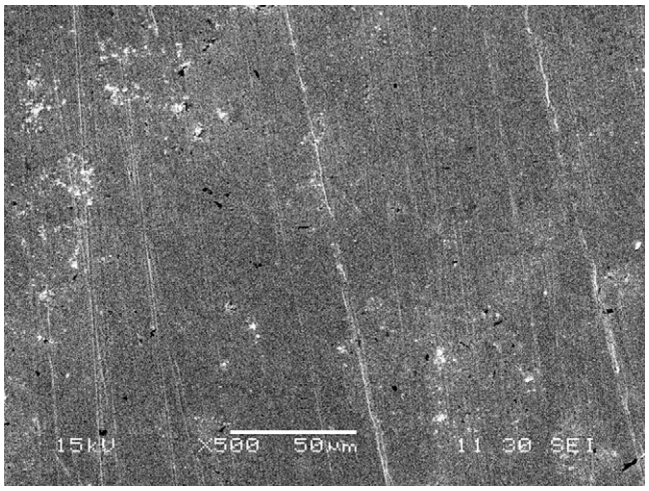

Fig. 9. Scanning electron micrograph (SEM) of metal surface after 7 days in CS + [NO_2^-] = 0.2 mol l^{-1} at open circuit potential (500×).

times higher than a single corresponding to carbon atoms, can be taken as an indication of the formation and presence of green rust carbonate on the carbon steel surface [11]. In Fig. 8 the absence of these characteristic high intensity peaks shows no green rust carbonate formation. The addition of 0.1 mol l^{-1} Cl$^-$ ions did not change the position and intensity of the EDX peaks. The absence of peaks corresponding to nitrogen atoms indicates that nitrite ions are not incorporated to the passive layer.

Fig. 10 shows photographs of the coupons after a 30 days period of immersion in each electrolyte, as indicated. The corrosion current values (j_{corr}) were calculated from weight loss results using the Faraday relationship [45]:

$$j_{corr} = \frac{mF}{At\,eq} \quad (6)$$

Table 4
Weight loss result after 30 days of immersion to the open circuit potential in the different solutions tested.

Pore solution	j_{corr} (A cm^{-2})	Type of attack	Inhibition (%)	[NO_2^-]/[Cl$^-$]
CS	2.3×10^{-6}	Red spots	–	–
CS + 2.5×10^{-4} mol l^{-1} NO_2^-	2×10^{-6}	Red spots	13	–
CS + 0.025 mol l^{-1} NO_2^-	6.7×10^{-8}	Red spots	97.1	–
CS + 0.2 mol l^{-1} NO_2^-	3.3×10^{-8}	Colorless surface	98.6	–
CS + 1×10^{-3} mol l^{-1} Cl$^-$	4.5×10^{-6}	Red spots	–	0
CS + 1×10^{-3} mol l^{-1} Cl$^-$ + 2.5×10^{-4} mol l^{-1} NO_2^-	2×10^{-6}	Red spots	33	0.25
CS + 1×10^{-3} mol l^{-1} Cl$^-$ + 0.2 mol l^{-1} NO_2^-	3.3×10^{-8}	Colorless surface	99.3	200
CS + 0.1 mol l^{-1} Cl$^-$	2.3×10^{-5}	Red spots	–	0
CS + 0.1 mol l^{-1} Cl$^-$ + 0.025 mol l^{-1} NO_2–	6.4×10^{-7}	Pitting	98.9	0.25
CS + 0.1 mol l^{-1} Cl$^-$ + 0.2 mol l^{-1} NO_2^-	2.5×10^{-8}	Colorless surface	99.8	2

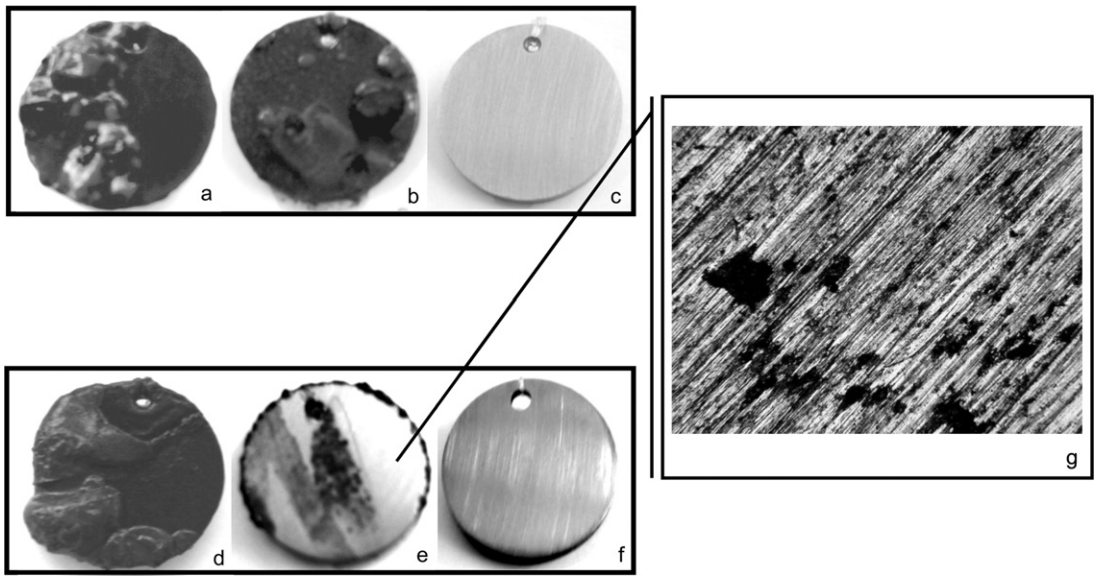

Fig. 10. Photographs of coupons after performing weight loss assay when $[Cl^-]/[OH^-] = 100$: (a) $[NO_2^-]/[Cl^-] = 0$, (b) $[NO_2^-] = 2.5 \times 10^{-4}$ mol l^{-1} or $[NO_2^-]/[Cl^-] = 0.25$ and (c) $[NO_2^-] = 0.2$ mol l^{-1} or $[NO_2^-]/[Cl^-] = 200$. Photographs of coupons after performing weight loss assay at $[Cl^-]/[OH^-] = 1 \times 10^4$: (d) $[NO_2^-]/[Cl^-] = 0$, (e) $[NO_2^-] = 0.025$ mol l^{-1} or $[NO_2^-]/[Cl^-] = 0.25$, (f) $[NO_2^-] = 0.2$ mol l^{-1} or $[NO_2^-]/[Cl^-] = 2$ and (g) coupon micrograph after chemical cleaning (100×) to $[NO_2^-] = 0.025$ mol l^{-1} or $[NO_2^-]/[Cl^-] = 0.25$.

where m is the mass loss, F is the Faraday constant, A is the exposed area, t is the exposition time and eq is the equivalent weight = 27.92 g.

The percentage of inhibition is calculated using the following equation

$$\text{Inhibition\%} = \left[1 - \left(\frac{j_{corr}\ \text{with inhibitor}}{j_{corr}\ \text{without inhibitor}}\right)\right] \times 100 \qquad (7)$$

The results are presented in Table 4.

Although, the percentage of inhibition calculated by means of j_{corr} values is more accurate, the values presented in Tables 1 and 2 calculated using Eq. (3) are in good agreement with the values shown in Table 4.

In highly alkaline solutions, the j_{corr} values typical of passive steel are close to 2×10^{-7} A cm^{-2} [46,47], while values higher than 1×10^{-6} A cm^{-2} are typical of the active state [30,48].

In CS the metal surface undergoes general corrosion. The degree of attack decreases when the nitrite ions content increases, and $[NO_2^-] = 0.2$ mol l^{-1} is necessary to attain a protective passive layer with an inhibition degree close to 99%.

When $[Cl^-]/[OH^-] = 100$, $[NO_2^-]/[Cl^-] = 0.25$ is not enough to improve the resistance to general corrosion. Only when $[NO_2^-]/[Cl^-] = 200$ the surface is passive with an inhibition degree of 99.3%. No pitting attack was detected ($[NO_2^-] = 0.2$ mol l^{-1}) after 30 days of immersion.

When $[Cl^-]/[OH^-] = 1 \times 10^4$, if $[NO_2^-]/[Cl^-] = 0.25$, the inhibition degree was 98.9%, but the coupons presented pitting. Only when $[NO_2^-]/[Cl^-] = 2$ the surface is passive with an inhibition degree of 99.8 and no pitting was detected after 30 days ($[NO_2^-] = 0.2$ mol l^{-1}).

4. Conclusions

In CS, with a low degree of carbonation, the steel surface undergoes general corrosion. When nitrite ions are present in high-enough concentrations they are responsible for the surface passivity, stabilizing an oxide film mainly composed of Fe_3O_4 and δ-FeOOH.

In the presence of nitrite and chloride ions a thicker and more compact passive layer develops on the electrode surface as the inhibitor content increases. The composition of this layer is similar to that found in the absence of chloride ions but, in this last case, pitting attack is observed. Independently of the chloride content, carbon steel presents the best behavior when $[NO_2^-] = 0.2$ mol l^{-1}, as lower nitrite dosages are not effective in preventing surface repassivation after pitting attack. At high chloride ions concentration, when inadequate dosages of inhibitor are used, the risk of pitting attack is high because E_{pit} is close to the OCP.

When carbon steel is in contact with CS where $[Cl^-]/[OH^-] = 100$ and $[NO_2^-]/[Cl^-] = 200$, the smallest j_{pas} and j_{corr} are measured. Also, E_{rp} is higher than E_{corr}. If $[Cl^-]/[OH^-] = 1 \times 10^4$ a $[NO_2^-]/[Cl^-]$ ratio of 2 is needed to produce the same result. In this way, the $[NO_2^-]/[Cl^-]$ ratio is not an appropriate parameter to evaluate the inhibitor efficiency at different chloride ions concentration in carbonated concrete. Although, the pitting potential shows a relativity good logarithmic correlation with this ratio, the difference $E_{pit} - E_{corr}$ was constant as nitrite ions concentration increased for the two chloride ions concentration tested.

At low chloride ions concentration, the metal surface undergoes general corrosion with a $[NO_2^-]/[Cl^-]$ ratio of 0.25 while, at higher chloride ions concentration a "poorly protective" passive layer is developed. On the other hand, in a previous work [8] it has been shown that a nitrite/chloride ratio of 0.25 or $[NO_2^-] = 0.2$ mol l^{-1} was necessary to induce complete surface repassivation of the metal in high alkaline solution (AS) ($[Cl^-]/[OH^-] = 1$). Thus, an optimal nitrite ions concentration ($[NO_2^-] = 0.2$ mol l^{-1}) can be established as the most suitable parameter to guarantee the inhibitor efficiency in the different electrolytes studied.

In CS the surface passivity at a fixed pH value is related to the CO_3^{2-} and HCO_3^- contents, where the effect of changing the HCO_3^-/CO_3^{2-} ratio is currently under investigation.

Acknowledgements

This work has been supported by the University of Mar del Plata (Grant 15/G150), as well as by the National Research Council (CONICET, PIP6252) and the Agencia Nacional de Promoción Científica y Tecnológica (PICTO 762/04). The assistance of the Centro de Microscopía Electrónica from the Universidad Nacional de Mar del Plata is greatly acknowledged.

References

[1] C.L. Page, V.T. Ngala, M.M. Page, Magazine of Concrete Research 52 (2000) 25.
[2] J.M. Gaidis, Cement & Concrete Composites 26 (3) (2004) 181.
[3] A.M. Rosemberg, J.M. Gaidis, Materials Performance 18 (11) (1979) 45.
[4] M. Saremi, E. Mahallati, Cement & Concrete Research 32 (2002) 1915.
[5] B. Elsener, Corrosion inhibitors for steel in concrete. State of the Art Report, EFC Publication 35, The Institute of Materials, Maney Publishing, London, 2001.
[6] K.Y. Ann, H.S. Jung, H.S. Kim, S.S. Kim, H.Y. Moon, Cement & Concrete Research 36 (3) (2006) 530.
[7] N.S. Berke, M.C. Hicks, Cement & Concrete Composites 26 (2004) 191.
[8] M.B. Valcarce, M. Vazquez, Electrochimica Acta 53 (15) (2008) 5007.
[9] L. Dhouibi, P. Refait, E. Triki, J.M.R. Génin, Journal of Materials Science 41 (2006) 4928.
[10] M. Refass, R. Sabot, M. Jeannin, P. Refait, Electrochimica Acta 52 (27) (2007) 7599.
[11] M.A. Deyab, S.S.A. El-Rehim, Electrochimica Acta 53 (2007) 1754.
[12] D.J. Anstice, C.L. Page, M.M. Page, Cement & Concrete Research 35 (2005) 377.
[13] S. Sawada, J. Kubo, C.L. Page, M.M. Page, Corrosion Science 49 (2007) 1186.
[14] M.C. Alonso, M.C. Andrade, Corrosion Science 29 (9) (1989) 1129.
[15] S.B. Farina, G.S. Duffó, Electrochimica Acta 52 (2007) 5131.
[16] M. Moreno, W. Morris, M.G. Alvarez, G.S. Duffo, Corrosion Science 46 (11) (2004) 2681.
[17] L. Li, A.A. Sagues, N. Poor, Cement & Concrete Research 29 (3) (1999) 315.
[18] M. Stern, A.L. Geary, Journal of the Electrochemical Society 104 (1957) 56.
[19] American Society of Testing and Materials, ASTM G61-86 Philadelphia, 1993.
[20] A. Palit, S. Pehkonen, Corrosion Science 42 (2000) 1801.
[21] J. Shim, J. Kim, Materials Letters 58 (2004) 2002.
[22] I. Scribner Associates, ZPlot for Windows. 1998.
[23] L.J. Aljinovic, S. Gudic, M. Smith, Journal of Applied Electrochemistry 30 (2000) 973.
[24] F. Foulkes, P. McGrath, Cement & Concrete Research 29 (1999) 873.
[25] S.T. Amaral, E.M.A. Martini, I.L. Muller, Corrosion Science 43 (5) (2001) 853.
[26] B. Huet, V. LïHostis, F. Miserque, H. Idrissi, Electrochimica Acta 51 (2005) 172.
[27] S.J. Harjac, A. Atrens, C.J. Moss, V. Linton, Journal of Materials Science 42 (2007) 9940.
[28] M. Pourbaix, Atlas of Electrochemical Equilibria in Aqueous Solutions, Pergamonn Press, Cebelcor, Brussels, 1974.
[29] C. Alonso, M. Castellote, C. Andrade, Electrochimica Acta 47 (21) (2002) 3469.
[30] M.F. Hurley, J.R. Scully, Corrosion (October) (2006) 892.
[31] C. Alonso, C. Andrade, M. Castellote, P. Castro, Cement & Concrete Research 30 (7) (2000) 1047.
[32] D.A. Hausmann, Journal of Materials Protection 11 (1967) 19.
[33] V.K. Gouda, British Corrosion Journal 5 (8) (1970) 198.
[34] A. Saraby-Reintjes, Electrochimica Acta 30 (3) (1985) 403.
[35] J.D. Kim, S.I. Pyum, Corrosion Science 38 (7) (1996) 1093.
[36] M. Yamaguchi, H. Nishihara, K. Aramaki, Corrosion Science 37 (4) (1995) 571.
[37] Y.M. Tang, Y. Zuo, X.H. Zhao, Corrosion Science 50 (2008) 989.
[38] V.S. Sastri, Corrosion Inhibitors. Principles and Applications, John Wiley & Sons, West Sussex, England, 1998.
[39] M.E. Orazem, B. Tribollet, Electrochemical Impedance Spectroscopy, John Wiley & Sons, New Jersey, 2008.
[40] J. Liu, D.D. Macdonald, Journal of the Electrochemical Society 148 (2001) B425.
[41] A. Carnot, I. Frateur, S. Zanna, B. Tribollet, I. Dubois-Brugger, P. Marcus, Corrosion Science 45 (2003) 2513.
[42] Z. Lu, D.D. Macdonnald, Electrochimica Acta 53 (2008) 7696.
[43] C. Andrade, M. Keddam, X.R. Novoa, M.C. Perez, C.M. Rangel, H. Takenouti, Electrochimica Acta 46 (24–25) (2001) 3905.
[44] S. Joiret, M. Keddam, X.R. Novoa, M.C. Pérez, C. Rangel, H. Takenouti, Cement & Concrete Composites 24 (2002) 7.
[45] American Society of Testing and Materials, ASTM G102-89 Philadelphia, 1994.
[46] J.A. Gonzalez, E. Ramirez, A. Bautista, S. Feliu, Cement & Concrete Research 26 (3) (1996) 501.
[47] A. Poursaee, C.M. Hansson, Cement & Concrete Research 37 (2007) 1127.
[48] J.A. Gonzalez, J.M. Miranda, N. Birbilis, S. Feliu, Corrosion 61 (1) (2005) 37.